Received: 19 April 2022 | Revised: 27 July 2022 | Accepted: 14 August 2022

IET Cyber-Systems and Robotics

DOI: 10.1049/csy2.12060

ZHEJIANG UNIVERSITY PRESS | The Institution of Engineering and Technology | WILEY

ORIGINAL RESEARCH

A hybrid tracking control strategy for an unmanned underwater vehicle aided with bioinspired neural dynamics

Zhe Xu[1] | Tao Yan[1] | Simon X. Yang[1] | S. Andrew Gadsden[2]

[1]School of Engineering, University of Guelph, Guelph, Ontario, Canada

[2]Department of Mechanical Engineering, McMaster University, Hamilton, Ontario, Canada

Correspondence

Simon X. Yang, School of Engineering, University of Guelph, Guelph, ON N1G 2W1, Canada.
Email: syang@uoguelph.ca

Funding information

Natural Sciences and Engineering Research Council of Canada

Abstract

Tracking control has been a vital research topic in robotics. This paper presents a novel hybrid control strategy for an unmanned underwater vehicle (UUV) based on a bioinspired neural dynamics model. An enhanced backstepping kinematic control strategy is first developed to avoid sharp velocity jumps and provides smooth velocity commands relative to conventional methods. Then, a novel sliding mode control is proposed, which is capable of providing smooth and continuous torque commands free from chattering. In comparative studies, the proposed combined hybrid control strategy has ensured control signal smoothness, which is critical in real-world applications, especially for a UUV that needs to operate in complex underwater environments.

KEYWORDS

backstepping, bioinspired neural dynamics, sliding mode control, unmanned underwater vehicle

1 | INTRODUCTION

The research on unmanned underwater vehicles (UUVs) has been ongoing for many years [1–7]. There are wide applications for UUVs, such as ocean surveillance, fishing, and submarine construction surveys. Tracking control has always been a fundamental issue in UUV research, although there are many other challenging issues [8, 9].

The studies on trajectory tracking control have been a major focus for autonomous vehicles. This research can be categorised primarily into four different methods: backstepping control [10, 11], sliding mode control [12–15], linearisation control [16, 17], and neural networks and fuzzy logic control [18–21]. The linearisation control method [16, 22] is straight forward and easy to implement; however, this method faces difficulty when applied to UUVs. These difficulties arise due to the complex environments in which UUVs usually operate, which makes the hydrodynamic forces hard to obtain.

The backstepping control method [23–25] is one of the most commonly used control methods in robot control. The design of backstepping control aims to recursively stabilise a closed loop feedback system, which is relatively easy to design and prove using Lyapunov stability theory. In addition, the backstepping control method has been adopted in UUV control design; however, the velocity control law is related to the tracking errors; therefore, the control signal will generate large initial velocity jumps if the initial tracking error is large. This large initial velocity change indicates that the UUV requires an impractical amount of torque to reach such velocities at the initial stage.

Sliding mode control [14, 26, 27] on UUVs has many advantages, such as insensitivity to parameter variances and providing the system with extra robustness against disturbances. The downside of the sliding mode control design is that this control method has the chattering issue, and these high frequency changes in the control signal may damage the hardware in UUVs. The aforementioned velocity jump issue in backstepping control and chattering issue in sliding mode control could be addressed using fuzzy logic control, which is another practical solution. However, fuzzy logic control [20, 21] requires human knowledge, and it is difficult to generate fuzzy rules that give satisfactory results. Neural networks [28, 29] are another solution that has been implemented on UUV controls, which has been used to compute the complex nonlinear relations from ocean disturbances. However, this method requires online learning and training processes, which could be expensive and computationally complicated.

The bioinspired neural dynamics model was first proposed by Hodgkin and Huxley [30] based on a patch of membrane in a biological neural system using electrical circuit elements. Then, this bioinspired neural dynamic model was first used by Yang [31] in robotics, which was later expanded into many other applications [32–34]. In the following work from Zhu [23], this bioinspired neural dynamic model was implemented on a kinematic control for a UUV in path tracking problems. The entire control design was a hybrid control, which used a bioinspired kinematic controller to resolve the speed jump issue in conventional backstepping (CB) control and a sliding mode controller for the dynamic control of the UUV.

Inspired by the special characteristic of bioinspired neural dynamics, this paper designs a bioinspired sliding mode controller that is capable of resolving the chattering issue, which is more practical in real-world applications. The chattering issue has existed since sliding mode control was developed, which can be observed from many applications. Although the chattering issue has been solved, such as using saturation or tanh function to replace the chattering term, there are still some drawbacks to the existing solutions, such as losing the robustness to the disturbances and the parameters have to be perfectly tuned to prevent chattering; in addition, considering the noises, the CB and sliding mode control are sensitive to the noises, whereas the bioinspired-based controller is capable of providing smooth control command, which is critical due to the limitations of the actuator.

Therefore, in this paper, a novel hybrid control method aided with the bioinspired neural dynamics model is proposed based on the preliminary work in Ref. [35]. This overall design contains a kinematic controller and a dynamic controller that are integrated with the bioinspired neural dynamics model. The proposed bioinspired kinematic controller is capable of avoiding the velocity jump. Then, to avoid the chattering issue in conventional sliding mode control, the same bioinspired neural dynamics is combined with the sliding mode control to provide continuous and smooth dynamic control output that is free from chattering. In addition, the proposed control strategy is capable of providing smooth control commands under the system and measurement noises due to the filtering capability from the bioinspired neural dynamics.

This paper is organised as follows: Section 2 provides the kinematic and dynamic model of a UUV operating underwater. Then, Section 3 provides the bioinspired neural dynamics model that helps to develop the bioinspired backstepping kinematic controller and bioinspired sliding mode controller. The stability analysis of the proposed control strategy is provided in Section 3 as well. The Section 4 gives the results, which are compared with multiple other methods to demonstrate its efficiency and effectiveness. Finally, the conclusion in Section 5 illustrates the developed concept and why the proposed control method is a better control strategy for a UUV. Some potential future improvements are also mentioned in the conclusion.

2 | KINEMATICS AND DYNAMICS OF A UUV

The UUVs dynamic model is presented as [36]

$$M\dot{V} + C(V)V + D(V)V + g(\eta) = \tau \tag{1}$$

where M is the inertial matrix, C is the Coriolis and centrifugal forces, and D is the hydrodynamic force. The UUVs gravity and buoyancy forces are represented by g. Figure 1 demonstrates the coordinate systems for UUV. The inertial frame of the UUV is represented by $\{X, Y, Z, O\}$ and $\{X_0, Y_0, Z_0, O_0\}$ is the coordinate of the body fixed frame coordinate system. The position and orientation of the UUV in the inertial frame is represented by vector $\eta = [x \quad y \quad z \quad \phi \quad \theta \quad \psi]^T$, where x, y, and z are the position and ϕ, θ, and ψ are the orientation in X, Y, and Z, respectively. The velocity vector of the UUV in body fixed frame is represented by $V = [u \quad v \quad w \quad p \quad q \quad r]^T$, where the elements in V are the surge, sway, heave, roll, pitch, and yaw motions of the UUV. The controlled torque is defined as τ that acts on the mass centre of the UUV.

The kinematics of the UUV is given as

$$\dot{\eta} = J(\eta)V \tag{2}$$

where $J(\eta)$ is a transformation matrix between the body fixed frame and inertial frame. This paper discusses the UUV that operates in horizontal plane; therefore, the reduced dynamics of the UUV can be written in a decoupled form as [37]

$$\tau_x = (m - X_{\dot{u}})\dot{u} + X_u u + X_{uu} u|u| \tag{3}$$

$$\tau_y = (m - Y_{\dot{v}})\dot{v} + Y_v v + Y_{vv} v|v| \tag{4}$$

$$\tau_N = (I_z - N_{\dot{r}})\dot{r} + N_r r + N_{rr} r|r| \tag{5}$$

where m represents the mass, and added mass effects of u and v are $X_{\dot{u}}$ and $Y_{\dot{v}}$, respectively. Parameter $N_{\dot{r}}$ is the added

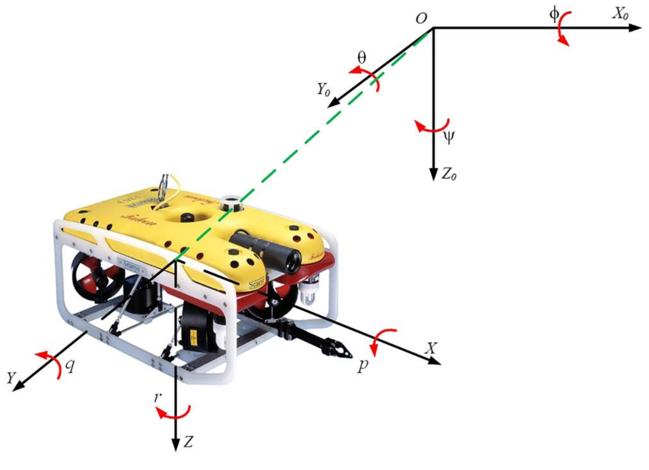

FIGURE 1 Unmanned underwater vehicle (UUV) coordinates in body fixed and inertial frame

moment of inertia from r, and I_z is the moment of inertia in z. Linear drag in u, v, and r, are, respectively, X_u, Y_v, and N_r. The quadratic drags in u, v, and r are X_{uu}, Y_{vv}, and N_{rr}, respectively. Vector $\tau = \begin{bmatrix} \tau_x & \tau_y & \tau_N \end{bmatrix}^{\mathrm{T}}$ is the control force and moment that is applied on the centre of mass on UUV in X, Y and orientation of body fixed frame.

3 | UUV CONTROL DESIGN AIDED WITH BIOINSPIRED NEURAL DYNAMICS

This section develops a hybrid control strategy for a UUV. The block diagram in Figure 2 demonstrates the designed control, which is a hybrid control strategy that consists of two closed loops. The outer loop consists of a bioinspired backstepping (BB)-based kinematic controller that is capable of providing smooth velocity command and preventing sharp velocity jumps from sudden changes in initial tracking errors. Then, the output control command from the BB controller is processed through the inner loop control, which is a sliding mode controller that is also combined with the bioinspired neural dynamics. The bioinspired sliding mode controller is capable of preventing the chattering issue that occurs in conventional sliding mode control yet a certain amount of robustness to disturbances remains as the bioinspired neural dynamics acts like a low pass filter.

3.1 | Bioinspired neural dynamic model

Hodgkin and Huxley [30] proposed a membrane model based on a path of a membrane using electrical elements. This model was then developed by Grossberg [38] who described a real-time adaptive behaviour of individuals. Then, it was first applied in robotics by Yang and Meng [31], which has been expanded into many other robotic applications. The bioinspired inspired neural dynamic model, which is called the shunting model, is written as

$$\dot{x}_i = -A_i x_i + (B_i - x_i)S_i^+ - (D_i + x_i)S_i^- \qquad (6)$$

where x_i is the neural activity of ith neuron, A_i is the passive decay rate, and B_i and D_i are the upper bound and lower bound of the ith neuron, respectively. Variables S_i^+ and S_i^- are the ith neuron excitatory and inhibitory inputs. Based on Equation (6), the shunting model that is applied in this paper is defined as

$$\dot{L}_i = -A_i L_i + (B_i - L_i)f(e_i) - (D_i + L_i)g(e_i) \qquad (7)$$

where e_i is the error between the reference state and the actual state of the UUV, which is treated as input of the bioinspired neural dynamics, and $f(e_i)$ and $g(e_i)$ are defined as $f(e_i) = \max(e_i, 0)$ and $g(e_i) = \max(-e_i, 0)$, respectively. Variable L_i is the output, which is guaranteed to be bounded within $(-D_i, B_i)$ for any input of e_i. In addition, it is worth noting that the shunting model also has the filtering property that acts like a low pass filter. Equation (7) is applied twice in this paper to separately address the velocity jump and chattering issues in backstepping control and sliding mode control. Inspired by the special characteristic of the shunting model, the following subsections explain the design procedures in detail.

3.2 | Bioinspired backstepping kinematic control

The backstepping control design is straightforward and relatively easy to design. This paper discusses the motion of a UUV in horizontal plane; therefore, for a UUV operating horizontally, the reference posture of a UUV is defined as $\eta_r = \begin{bmatrix} x_r & y_r & \psi_r \end{bmatrix}^T$ in inertial frame. The desired reference velocity state in surge, sway, and yaw motions is defined as $V_r = \begin{bmatrix} u_r & v_r & r_r \end{bmatrix}^T$. Based on Equation (2), the relations between the reference position state and reference velocity state can be obtained through a transformation matrix $J(\eta)$, which is defined as

$$\begin{bmatrix} u_r \\ v_r \\ r_r \end{bmatrix} = \begin{bmatrix} C\psi_r & S\psi_r & 0 \\ -S\psi_r & C\psi_r & 0 \\ 0 & 0 & 1 \end{bmatrix} \begin{bmatrix} \dot{x}_r \\ \dot{y}_r \\ \dot{r}_r \end{bmatrix} \qquad (8)$$

where S and C represent sin and cos function, respectively. The objective of the kinematic controller is to generate velocity control commands, which forces the UUV to reach a certain velocity that makes the tracking error approach zero. The tracking error with respect to the body fixed frame is defined as $e_P = \begin{bmatrix} e_1 & e_2 & e_3 \end{bmatrix}^T$, where e_1, e_2, and e_3 are the tracking error in surge, sway, and yaw motion with respect to the body fixed frame. The tracking error with respect to inertial frame is calculated by

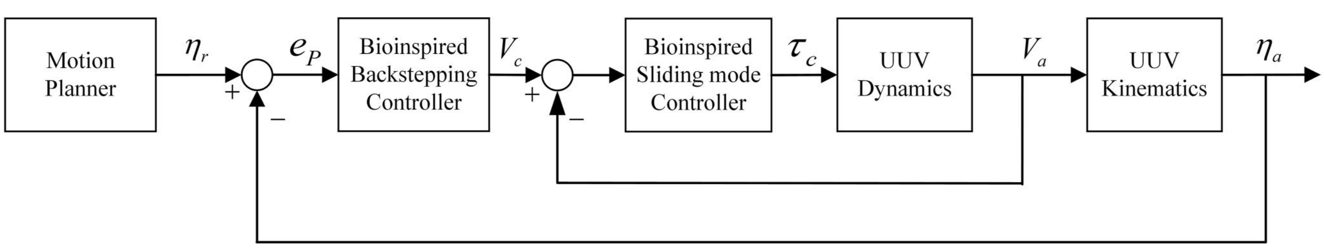

FIGURE 2 Block diagram of an UUV based on the bioinspired control strategy

$$e_P = J(\eta)^{-1}\begin{bmatrix} e_x & e_y & e_\psi \end{bmatrix}^T \tag{9}$$

Figure 3 shows the coordinate conversion of the tracking error between the body fixed frame and inertial frame, where e_x, e_y, and e_ψ are, respectively, the tracking error in X, Y and orientation in inertial frame. Then, the convectional design of the back stepping-based kinematic control for the UUV is given as

$$V_c = \begin{bmatrix} u_c & v_c & r_c \end{bmatrix}^T = \begin{bmatrix} k_a\left(e_x C(\psi) + e_y S(\psi)\right) + \left(u_r S\left(e_\psi\right) - v_r C\left(e_\psi\right)\right) \\ k_a\left(-e_x S(\psi) + e_y C(\psi)\right) + \left(u_r S\left(e_\psi\right) + v_r C\left(e_\psi\right)\right) \\ r_d + k_b e_\psi \end{bmatrix} \tag{10}$$

The velocity commands in the surge, sway, and yaw motions are u_c, v_c and r_c, respectively. Parameters k_a and k_b are the control parameters for the backstepping-based kinematic controller. Based on Equation (10), it can be observed that if there is a large tracking error at the initial stage, $e_x C(\psi) + e_y S(\psi)$, $-e_x S(\psi) + e_y C(\psi)$, and $k_b e_\psi$ will cause speed jumps in surge, sway, and yaw motions, respectively. Therefore, in order to resolve the speed jump issue, the BB control is proposed, in which the new virtual velocity command is defined as

$$V_c = \begin{bmatrix} u_c & v_c & r_c \end{bmatrix}^T = \begin{bmatrix} k_a(L_1 C(\psi) + L_2 S(\psi)) + \left(u_r S\left(e_\psi\right) - v_r C\left(e_\psi\right)\right) \\ k_a(-L_1 S(\psi) + L_2 C(\psi)) + \left(u_r S\left(e_\psi\right) + v_r C\left(e_\psi\right)\right) \\ r_r + k_b L_3 \end{bmatrix} \tag{11}$$

where L_1, L_2 and L_3 are the outputs from the bioinspired neural dynamics whereas e_x, e_y and e_ψ are the respected inputs. Due to the special characteristics of the shunting model, by assuming $B_i = D_i$, the error term in the virtual control commands has the following inequalities

$$\begin{gathered} k_a(L_1 C(\psi) + L_2 S(\psi)) < k_a(B_1 + B_2) \\ k_a(-L_1 C(\psi) + L_2 S(\psi)) < k_a(-B_1 + B_2) \\ k_b L_3 < k_b B_3 \end{gathered} \tag{12}$$

where B_1, B_2, and B_3 are positive constants. Thus, by carefully selecting the u_r, v_r, and r_r, the velocity virtual control inputs are bounded and not exceeding its dynamic constraints. In addition, the BB control is also capable of providing smooth control input under noise due to its filtering capability; A_i in the shunting model acts as the bandwidth of the low pass filter. To prove the stability of the BB control, the Lyapunov candidate function is proposed as

$$V_p = \frac{1}{2}\left(e_x^2 + e_y^2 + e_\psi^2\right) + \frac{k_a}{2B_1}L_1^2 + \frac{k_a}{2B_2}L_2^2 + \frac{k_b}{2B_3}L_3^2 \tag{13}$$

then, the derivative of V_p is found to be

$$\dot{V}_p = e_x \dot{e}_x + e_y \dot{e}_y + e_\psi \dot{e}_\psi + \frac{k_a}{B_1}L_1\dot{L}_1 + \frac{k_a}{B_2}L_2\dot{L}_2 + \frac{k_b}{B_3}L_3\dot{L}_3 \tag{14}$$

The proposed bioinspired kinematic control strategy is capable of generating smooth velocity commands and avoiding sharp velocity jumps if an initial tracking error occurs, and its stability is proven in Subsection 3.4.

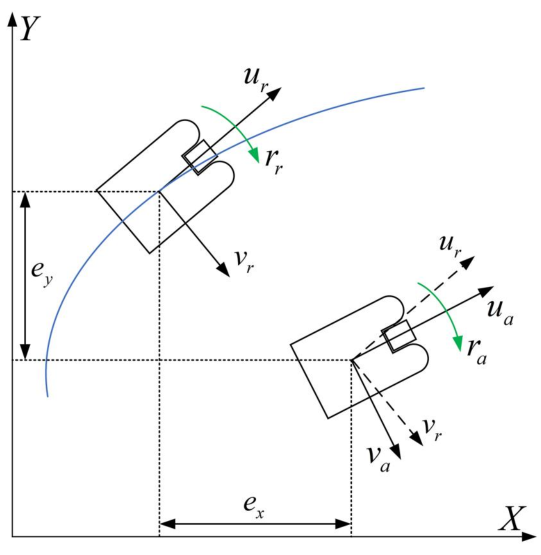

FIGURE 3 Coordinate conversion for unmanned underwater vehicle

3.3 | Bioinspired sliding mode dynamic control

This subsection develops a sliding mode controller that is aided with bioinspired neural dynamics aforementioned from Subsection 3.1. The generated virtual velocity commands from BB control are treated as the reference state for the dynamic control of the UUV. The control command τ is then generated from the bioinspired sliding model controller, which is used to drive the dynamic model of UUV to reach its desired state.

First, the velocity error is defined as $e = V_c - V_a$, where V_a is the actual velocity that is observed with respect to the body fixed frame. Defining Γ as a positive constant, the sliding surface is proposed as

$$S = \dot{e} + 2\Gamma e + \Gamma^2 \int e \tag{15}$$

By taking the derivative of Equation (15), which gives

$$\dot{S} = \ddot{e} + 2\Gamma\dot{e} + \Gamma^2 e = \ddot{e} + 2\Gamma\left(\dot{V}_c - \dot{V}_a\right) + \Gamma^2 e \tag{16}$$

Based on Equation (16), if the system operates on the sliding surface, then,

$$\dot{S} = \ddot{e} + 2\Gamma\left(\dot{V}_c - \dot{V}_a\right) + \Gamma^2 e = 0 \tag{17}$$

From Equation (1) into Equation (17), it is calculated as

$$\ddot{e} + 2\Gamma(\dot{V}_c - M^{-1}(\tau - CV_a - DV_a - g)) + \Gamma^2 e = 0 \tag{18}$$

Therefore, the equivalent control law is found that

$$\tau_{eq} = M\left(\dot{V}_c + \frac{\ddot{e}}{2\Gamma} + \frac{\Gamma}{2}e\right) + CV_a + DV_a + g \tag{19}$$

A feedback control input of acceleration is used in Equation (19) due to the difficulty of computing $\ddot{e}$, which is defined as

$$\ddot{e} = k_s\dot{e} \tag{20}$$

Therefore, the conventional sliding mode control law is defined as

$$\tau = \tau_{eq} + k\mathrm{sgn}(S) \tag{21}$$

It is observed from Equation (21) that the chattering in control signal is caused by sign function. One commonly used control method that is capable of eliminating the chattering issue in conventional sliding mode control is by replacing the sign function with saturation function. The sliding mode control with saturation function can be defined as

$$\tau = \tau_{eq} + \mathrm{Sat}(S)$$
$$\mathrm{Sat}(S) = \begin{cases} B_4 & \text{if} \quad k_sS > B_4 \\ k_sS & \text{if} \quad -D_4 \le k_sS \le B_4 \\ -D_4 & \text{if} \quad k_sS < -D_4 \end{cases} \tag{22}$$

where k_s is a positive constant that defines the changing rate of the control output, and B_4 and $-D_4$ are the upper bound and lower bound of the saturation function, respectively. Although the saturation function works in some situations if the control parameters are relatively small, UUVs usually operate in complicated environments, which sometimes require larger control parameters. Therefore, the same bioinspired neural dynamic that applied to the CB control in Equation (11) is combined with sliding mode control again. The bioinspired sliding mode control is defined as

$$\tau = \tau_{eq} + L_4 \tag{23}$$

where L_4 is the output of the shunting model that is defined in Equation (6). The Lyapunov candidate function for the bioinspired sliding mode controller is proposed as

$$V_z = \frac{1}{2}S^TS + \frac{1}{2B_4}{L_4}^TL_4 \tag{24}$$

Then, the derivative of Equation (24) is calculated as

$$\dot{V}_z = S^T\dot{S} + \frac{1}{B_4}\dot{L}_4{}^TL_4 \tag{25}$$

The proposed sliding mode dynamic control input solves the chattering issue that occurs in the conventional control method yet gives extra robustness to the controller since there are more parameters that can be tuned for the controller to reach satisfactory results.

3.4 | Stability analysis

The proposed control strategy contains two closed loops, which are BB kinematic control in the outer loop and bioinspired sliding mode control in inner loop. These two kinematic and dynamic controls are separately proven to be asymptotically stable using Lyapunov stability analysis. Then, an overall Lyapunov candidate function is provided to demonstrate that the proposed control strategy reaches global asymptotic stability.

For BB control, the time derivative of the Lyapunov candidate function in Equation (14) is divided into three components, which would be easier for the calculations. These three components are $e_x\dot{e}_x + e_y\dot{e}_y$, $\frac{k_a}{B_1}L_1\dot{L}_1 + \frac{k_a}{B_2}L_2\dot{L}_2$, and $e_\psi\dot{e}_\psi + \frac{k_b}{B_3}L_3L_3$. From the definition of the tracking errors, $e_x\dot{e}_x + e_y\dot{e}_y$ is rewritten as

$$e_x\dot{e}_x + e_y\dot{e}_y = e_x(x_r - x_a) + e_y(y_r - y_a) \tag{26}$$

Then, based on Equations (2) and (8), (26) is rewritten as

$$\begin{aligned} e_x\dot{e}_x + e_y\dot{e}_y = e_x\big((&C(\psi_d)u_d - S(\psi_d)v_d) \\ &- (u_aC(\psi_a) - v_aS(\psi_a))\big) \\ &+ e_y\big((S(\psi_r)u_r + C(\psi_r)v_r) \\ &- (u_aS(\psi_a) + v_aC(\psi_a))\big) \end{aligned} \tag{27}$$

By substituting Equation (11) into Equation (27), it can be calculated that

$$\begin{aligned} e_x\dot{e}_x + e_y\dot{e}_y &= e_x\big((C(\psi_r)u_r - S(\psi_r)v_r) \\ &\quad - (k_aL_1 + u_rC(\psi_r) + v_rS(\psi_r))\big) \\ &\quad + e_y\big((S(\psi_r)u_r + C(\psi_r)v_r) \\ &\quad - (k_aL_2 + u_rS(\psi_r) - v_rC(\psi_r))\big) \\ &= -k_ae_xL_1 - k_ae_yL_2 \end{aligned} \tag{28}$$

For the second part of the Lyapunov function for the BB controller, $\frac{k_a}{B_1}L_1\dot{L}_1 + \frac{k_a}{B_2}L_2\dot{L}_2$, by assuming $B_1 = D_1$ and $B_2 = D_2$, based on the definition of the shunting model in Equation (7), it is derived as

$$\begin{aligned} \frac{k_a}{B_1}L_1\dot{L}_1 + \frac{k_a}{B_2}L_2\dot{L}_2 = \frac{k_a}{B_1}&(-A_1 - f(e_x) - g(e_x))L_1^2 \\ &+ k_a(f(e_y) - g(e_y))L_1 \\ &+ \frac{k_a}{B_2}(-A_1 - f(e_y) - g(e_y)) \\ &\times L_2^2 + k_a(f(e_y) - g(e_y))L_2 \end{aligned} \tag{29}$$

The last part of Equation (14) is $e_\psi \dot{e}_\psi + k_b L_3 \dot{L}_3$, which is calculated as

$$e_\psi \dot{e}_\psi + \frac{k_3}{B_1} L_3 \dot{L}_3 = -k_b e_\psi L_3 + \frac{k_b}{B_3}\left(-A_3 - f\left(e_\psi\right) - g\left(e_\psi\right)\right) L_3^2 + k_b\left(f\left(e_\psi\right) - g\left(e_\psi\right)\right) L_3 \quad (30)$$

By combining Equations (28), (29) and (30), based on Equation (7), it can be concluded that $f(e_i) = e_i$ and $g(e_i) = 0$, if $e_i \geq 0$. Otherwise, if $e_i \leq 0$ then $g(e_i) = -e_i$ and $f(e_i) = 0$. It can be concluded in Equations (29) and (30) that

$$\begin{aligned} -A_i - f(e_i) - g(e_i) &\leq 0 \\ f(e_i) - g(e_i) - e_i &= 0 \end{aligned} \quad (31)$$

In addition, as $t \to \infty$ and $V_p \to 0$, overall, $\dot{V}_p$ is non-positive, if and only if e_x, e_y, and e_ψ are zeros, $V_p = 0$. Thus, the BB control is proven to be asymptotically stable.

As for the bioinspired sliding mode control, substituting Equations (7) and (17) into Equation (25), it gets

$$\dot{V}_z = S^T\left(\ddot{e} + 2\Gamma\dot{e} + \Gamma^2 e\right) + \frac{1}{B_4}\left(-A_4{}^T L_4{}^T + \left(B_4{}^T - L_4{}^T\right) f(S)^T - \left(D_4{}^T + L_4{}^T\right) g(S)^T\right) L_4 \quad (32)$$

Then, substituting Equations (1) and (19) into Equation (32), $\dot{V}_z$ becomes

$$\begin{aligned} \dot{V}_z = S^T L_4 &+ \frac{1}{B_4{}^T} L_4{}^T\left(-A_2{}^T - f(S)^T - g(S)^T\right) \\ &+ \frac{1}{B_4{}^T} L_4\left(B_4{}^T f(S)^T - D_4{}^T g(S)^T\right) L_4 \end{aligned} \quad (33)$$

By letting $B_4{}^T = D_4{}^T$, Equation (33) finally becomes

$$\begin{aligned} \dot{V}_z = &\frac{1}{B_4{}^T} L_4 L_4{}^T\left(-A_4{}^T - f(S)^T - g(S)^T\right) \\ &+ \left(f(S)^T - g(S)^T + S^T\right) L_4 \end{aligned} \quad (34)$$

Similar to the concept of Equation (31), it is obvious that $\frac{L_4 L_4{}^T}{B_4{}^T}\left(-A_4{}^T - f(S)^T - g(S)^T\right) \leq 0$ and $\left(f(S)^T - g(S)^T + S^T\right) = 0$. As $t \to \infty$, both L_4 and S approaches zero, only if e equals to zero, $S = 0$. In addition, using the input–output property of shunting model from Equation (7) as $e \to 0$, L_4 approaches zero as well.

For the overall stability, the Lyapunov candidate function and its time derivative are proposed as

$$\begin{aligned} V_o &= V_p + V_z \\ \dot{V}_o &= \dot{V}_p + \dot{V}_z \end{aligned} \quad (35)$$

Based on the results obtained from Equations (26) to (34), it is easy to verify that $V_o \leq 0$, if and only if e_x, e_y, e_ψ, and e are equal to zero, then $V_o = 0$. Thus, the overall control stability has been proven.

4 | RESULTS

This section demonstrates the superiority of the bioinspired aided controllers over the conventional method. The proposed control strategy generates smooth velocity and torque commands, which overcomes velocity overshoot and chattering problems in backstepping control and sliding mode control, respectively. Simulation results are shown in two different parts, tracking a straight path and a circular path, which are the two types of typical movements for a UUV operating underwater. In order to demonstrate the superiority of the proposed control strategy, three other methods are shown in the comparison. The UUV parameters [23, 39] are provided as $m - X_{\dot{u}} = m - Y_{\dot{v}} = 54.35$, $I_z - N_{\dot{r}} = 1.93$. The linear drag with respect to surge, sway, and yaw motion are treated as $X_u = Y_v = 17.51$, $N_r = 2.4$, finally, the quadratic drag for the UUV are $X_{uu} = 10$, $Y_{vv} = 10$, and $N_{rr} = 2$ in surge, sway, and yaw motions, respectively. The control variables are set to $k = [2 \quad 2 \quad 0.2]^T$, $k_a = 2$, $k_b = 1$, $k_s = 1$, and $\Gamma = 1$. As for the shunting model that is used in both backstepping and sliding mode control, the variables are set to $A_1 = A_2 = A_3 = 4$, $B_1 = B_2 = B_3 = D_1 = D_2 = D_3 = 1$, $A_4 = [3 \quad 3 \quad 3]^T$, and $B_4 = D_4 = [1 \quad 1 \quad 1]^T$. In addition, the saturation function used to replace the sign function in sliding is provided as $B_4 = D_4 = [1 \quad 1 \quad 0.03]^T$, and $k_s = 3$. The torque command follows the time response of the first order system to ensure its smoothness; then the actual torque commands generated are defined as $\tau_c(t) = \tau(t)\left(1 - e^{-t\sigma}\right)$, where τ_c is the actual command that is sent to the UUV dynamics and σ is set to 0.5. Finally, the sampling time is set to 0.01 s.

4.1 | Straight path tracking

One of the most common movements for a UUV operating underwater is to move straight forward; therefore, a straight path is given to test the efficiency and effectiveness of the proposed method; in addition, it is assumed that the desired tracking trajectory is continuous and differentiable. Given the desired tracking trajectory as $X_d = 3 + 0.4\ t$, $Y_d = 0.4\ t$, and $\psi_d = 45°$, the initial state for the UUV is set as (0, 0) and $\psi_a = 0$. Figure 4 shows that all the control strategies track desired trajectory, and the CB control strategy yields a slightly different path than other methods with BB control.

However, in Figure 5, the velocity commands that are generated from the CB control suffer from speed jump issues, whereas other control methods that are implemented with BB control yield smooth velocity commands without any speed jump. This speed jump issue is critical for UUVs in real-world applications, because a speed jump would infer that the initial

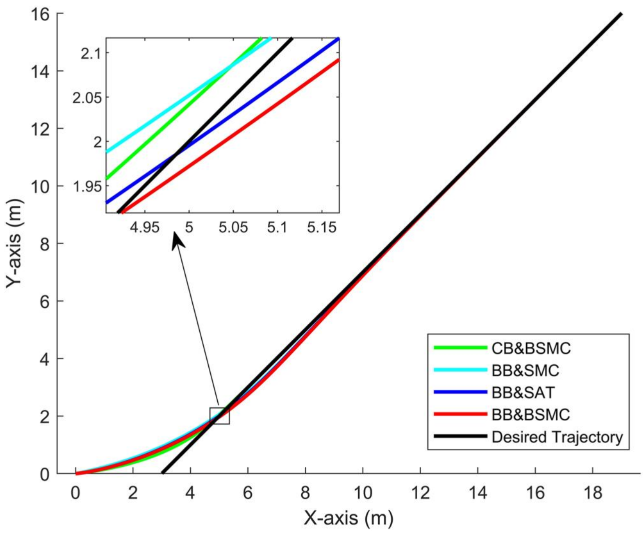

FIGURE 4 Straight path tracking trajectories. BB, Bioinspired backstepping; BSMC, Bioinspired sliding mode; CB, Conventional backstepping; SMC, Conventional sliding mode; SAT, Sliding mode with saturation

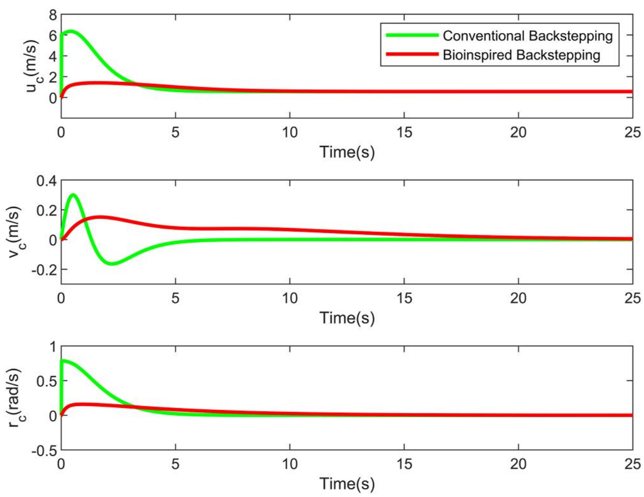

FIGURE 5 Velocity commands for unmanned underwater vehicle tracking a straight path. Green: Conventional backstepping; Red: Bioinspired backstepping

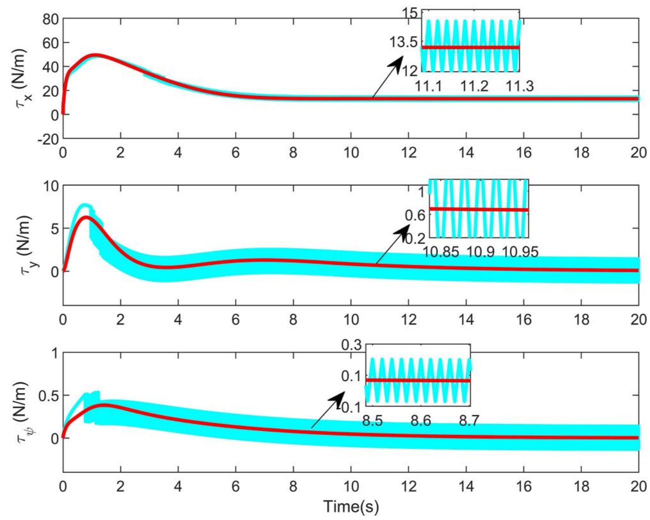

FIGURE 6 Torque commands for unmanned underwater vehicle tracking a straight path. Cyan: Conventional sliding mode control; Red: Bioinspired sliding mode control

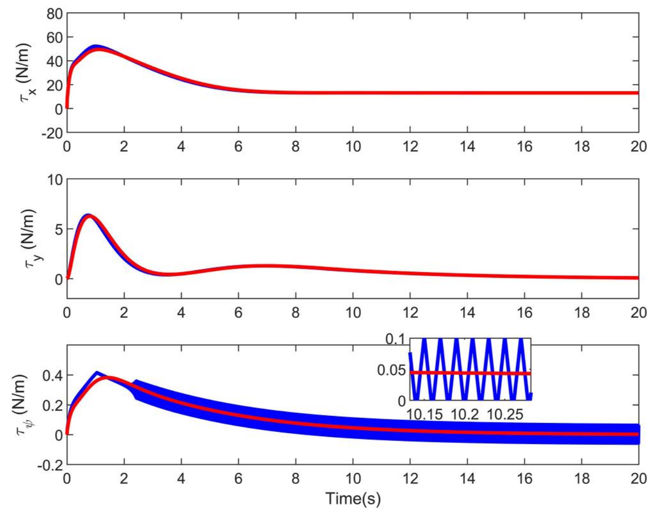

FIGURE 7 Torque command comparison for unmanned underwater vehicle tracking a straight path. Blue: sliding mode control with saturation function; Red: bioinspired sliding mode control

demanding torque would be infinitely large for a UUV to be able to reach such speed instantly. Therefore, the BB control has practically solved this issue. In addition, based on the observation in Figure 6, the sliding mode torque control suffers from the chattering issue whereas the bioinspired sliding mode control has avoided chattering and provides smooth control inputs.

The saturation function is a commonly used method that can be integrated with sliding mode control to eliminate the chattering issue in the conventional control method. Based on the definition of Equation (22), the saturation function could still potentially produce chattering problems if the tracking error does not fall between $[-D_4, B_4]$ and the k_s is not perfectly tuned. Since the UUV usually operates in complicated environments, the control parameters for sliding mode control with saturation function could be difficult to tune to give satisfactory results. As shown in Figure 7, although τ_x and τ_y are relatively smooth, there is still a chattering issue, which occurs in τ_ψ. Therefore, the saturation function does not completely resolve the chattering issue, but bioinspired sliding mode control is able to handle the chattering problem perfectly.

4.2 | Circular path tracking

This subsection tests the proposed tracking control strategy for a UUV tracking a circular path, which is a typical movement that UUVs need to achieve for trajectory tracking. The

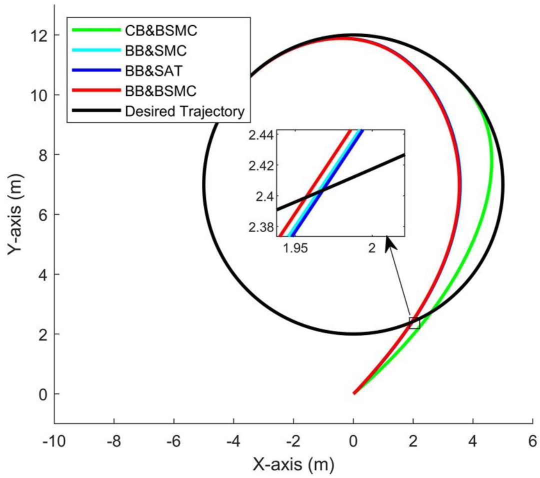

FIGURE 8 Circular trajectory tracking with different control strategies. BB, Bioinspired backstepping; BSMC: Bioinspired sliding mode; CB, Conventional backstepping; SAT, Sliding mode with saturation; SMC, Conventional sliding mode

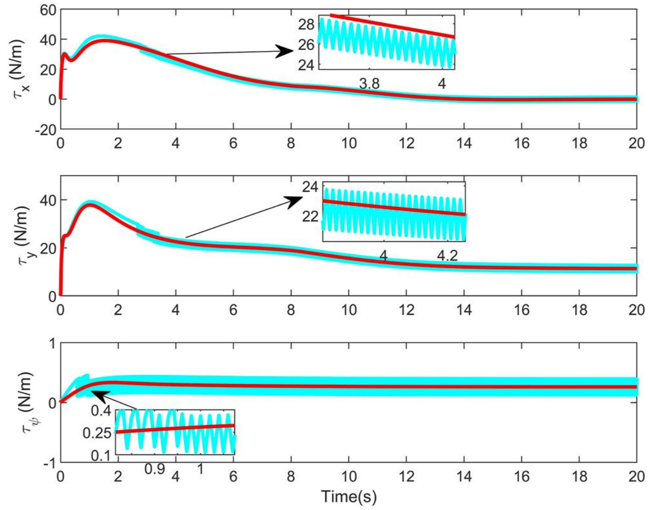

FIGURE 10 Torque commands for circular path tracking. Cyan: Conventional sliding mode control; Red: Bioinspired sliding mode control

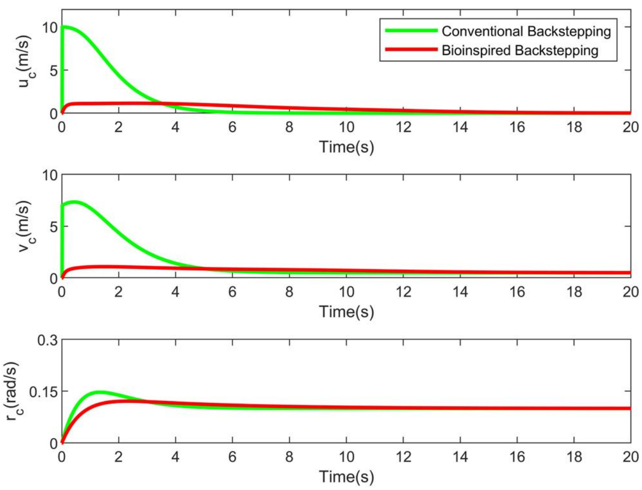

FIGURE 9 Torque commands for unmanned underwater vehicle tracking a circular path. Green: Conventional backstepping; Red: Bioinspired backstepping

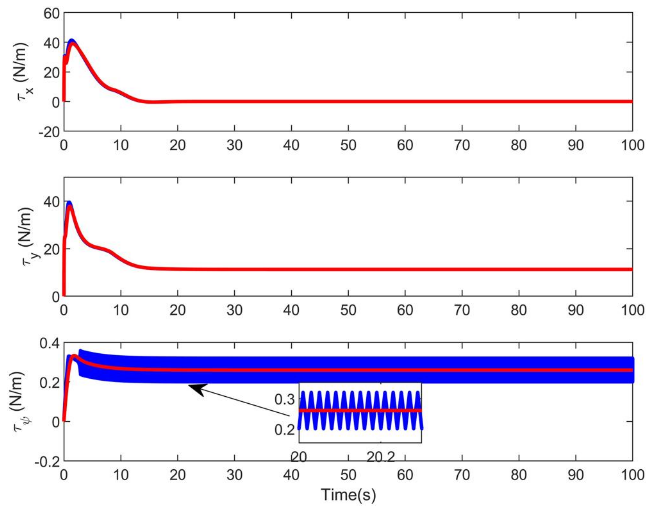

FIGURE 11 Torque command comparison for unmanned underwater vehicle tracking a circular path. Blue: Sliding mode control with saturation function; Red: Bioinspired sliding mode control

reference tracking path is defined as $X_r = 5\cos(0.1\ t)$, $Y_r = 7 + 5\sin(0.1\ t)$, and $\Psi_d = 0.1\ t$, and the starting state of the UUV is defined as (0, 0) and $\psi_a = 0$. The results are shown in Figure 8; all the tracking strategies make the UUV tracks the desired circular path. However Figure 9 once again shows that the BB control outperforms the CB control, and the BB control once again provides smooth velocity commands without sharp velocity changes whereas there is large velocity jumps from the conventional method.

The velocity commands from the BB control method and then propagates through the dynamic controller, where the results are shown in Figure 10. The output from the sliding mode controller suffers from the chattering issue, and the bioinspired sliding mode controller yields smooth torque commands. In addition, by comparing the results with the saturation function in Figure 11, it shows that tracking a circular path for a UUV does not remove the chattering issue in the saturation function, while bioinspired sliding mode control still yields satisfactory results. The proposed hybrid control strategy has proven to be the best choice over the other control strategies in the provided results.

4.3 | Tracking performance under noises

The UUV often operates in complex and complicated environments where the system and measurement noises play major roles in tracking performance, as well as the control smoothness. Thus, the proposed control strategy is tested under system and measurement noises. The Kalman filter and extended Kalman filter are, respectively, used to provide accurate state estimates for the kinematics and dynamics of the

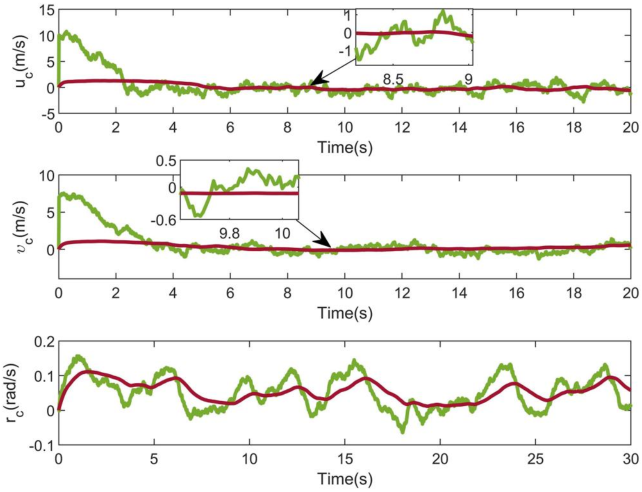

FIGURE 12 Velocity command comparison for unmanned underwater vehicle tracking a circular path under noises. Green: Conventional backstepping and sliding mode control with saturation function; Red: Bioinspired backstepping and bioinspired sliding mode controls

UUV. The system noises are considered as zero mean Gaussian with the covariance of $\left[10^{-3} \quad 10^{-3} \quad 10^{-4}\right]$ in the velocitie estimates, and $\left[10^{-5} \quad 10^{-5} \quad 10^{-6}\right]$ in the position state estimates. The measurement noises are treated as ten times higher than the system noises, respectively. The path that is used to test the tracking performance is a circular path same as Subsection 4.2, which is defined as $X_r = 5\cos(0.1\ t)$, $Y_r = 7 + 5\sin(0.1\ t)$, and $\Psi_d = 0.1\ t$, and the starting state of the UUV is defined as (0, 0) and $\psi_a = 0$.

As shown in Figure 12, under the noises, the proposed bioinspired control strategy is capable of providing a smooth velocity command, while the control signal in conventional method has a chattering issue under the noises. This control smoothness is critical since the actuator may not be able to handle fast changing signals, and the conventional method apparently places an extra burden on the actuator.

5 | CONCLUSIONS

This paper developed a hybrid control strategy for UUV; the proposed control strategy contains a BB kinematic controller and bioinspired sliding mode controller, which, respectively, resolves speed jumps and chattering issues in conventional design. In addition, the proposed strategy is capable of providing smooth control inputs even under system and measurement noises. To demonstrate the efficiency and effectiveness of the proposed method, a comprehensive comparison study is conducted; the results show that the proposed control strategy has more advantages over the other methods in terms of the tracking command smoothness and practicability. Further studies could potentially focus on resolving the effects of disturbances with accurate state estimates towards the proposed control strategy.

ACKNOWLEDGEMENTS

This work is supported by the Advanced Robotic Intelligent Systems Laboratory at the University of Guelph under Natural Sciences and Engineering Research Council of Canada (NSERC).

CONFLICT OF INTEREST

No potential conflict of interest was reported by the authors.

DATA AVAILABILITY STATEMENT

The research in this paper is conducted by simulations with the algorithms and parameters given in the paper. No real data are needed for this paper.

ORCID

Zhe Xu https://orcid.org/0000-0001-7227-640X
Tao Yan https://orcid.org/0000-0002-4494-9598
Simon X. Yang https://orcid.org/0000-0002-6888-7993
S. Andrew Gadsden https://orcid.org/0000-0003-3749-0878

REFERENCES

1. Zhang, Z., Wu, Y.: Adaptive fuzzy tracking control of autonomous underwater vehicles with output constraints. IEEE Trans. Fuzzy Syst. 14(8), 1–1 (2020). https://doi.org/10.1109/tfuzz.2020.2967294
2. Zhu, D., Zhou, B., Yang, S.X.: A novel algorithm of multi-AUVs task assignment and path planning based on biologically inspired neural network map. IEEE Trans Intell Veh. 6(2), 333–342 (2021). https://doi.org/10.1109/tiv.2020.3029369
3. Zhu, D., et al.: A hybrid control strategy of 7000 M-human occupied vehicle tracking control. IEEE Trans. Intell. Veh. 5(2), 251–264 (2020). https://doi.org/10.1109/tiv.2019.2955901
4. Zhu, D., Yang, S.X.: Bio-inspired neural network-based optimal path planning for UUVs under the effect of ocean currents. IEEE Trans. Intell. Veh. 7(2), 231–239 (2021). https://doi.org/10.1109/tiv.2021.3082151
5. He, S., et al.: Robust orientation-sensitive trajectory tracking of underactuated autonomous underwater vehicles. IEEE Trans. Ind. Electron. 68(9), 8464–8473 (2021). https://doi.org/10.1109/tie.2020.3013790
6. Tijjani, A.S., Chemori, A., Creuze, V.: Robust adaptive tracking control of underwater vehicles: design, stability analysis, and experiments. IEEE ASME Trans. Mechatron. 26(2), 897–907 (2021). https://doi.org/10.1109/tmech.2020.3012502
7. Gan, W., et al.: Model predictive adaptive constraint tracking control for underwater vehicles. IEEE Trans. Ind. Electron. 67(9), 7829–7840 (2020). https://doi.org/10.1109/tie.2019.2941132
8. Zhu, D., et al.: Multi-AUV hunting algorithm based on bio-inspired neural network in unknown environments regular paper. Int. J. Adv. Rob. Syst. 12(11), 1–12 (2015). https://doi.org/10.5772/61555
9. Ni, J., et al.: A dynamic bioinspired neural network based real-time path planning method for autonomous underwater vehicles. Comput. Intell. Neurosci. 2017, 1–16 (2017). https://doi.org/10.1155/2017/9269742
10. Liang, X., et al.: Three-Dimensional path following of an underactuated AUV based on fuzzy backstepping sliding mode control. Int. J. Fuzzy Syst. 20(2), 640–649 (2018). https://doi.org/10.1007/s40815-017-0386-y
11. Yang, S.X., et al.: A bioinspired neurodynamics-based approach to tracking control of mobile robots. IEEE Trans. Ind. Electron. 59(8), 3211–3220 (2012). https://doi.org/10.1109/tie.2011.2130491
12. Qiao, L., Zhang, W.: Trajectory tracking control of AUVs via adaptive fast nonsingular integral terminal sliding mode control. IEEE Trans. Ind. Inf. 16(2), 1248–1258 (2020). https://doi.org/10.1109/tii.2019.2949007
13. Wu, Z., et al.: Trajectory tracking of a novel underactuated AUV via nonsingular integral terminal sliding mode control. IEEE Access. 9, 103407–103418 (2021). https://doi.org/10.1109/access.2021.3098800

14. Manzanilla, A., et al.: Super-twisting integral sliding mode control for trajectory tracking of an Unmanned Underwater Vehicle. Ocean. Eng. 234, 109164 (2021). https://doi.org/10.1016/j.oceaneng.2021.109164
15. Zhu, C., et al.: Trajectory tracking control for autonomous underwater vehicle based on rotation matrix attitude representation. Ocean. Eng. 252(March 2021), 111206 (2022). https://doi.org/10.1016/j.oceaneng.2022.111206
16. Chwa, D.: Tracking control of differential-drive wheeled mobile robots using a backstepping-like feedback linearization. IEEE Trans. Syst. Man Cybern. Syst. Hum. 40(6), 1285–1295 (2010). https://doi.org/10.1109/tsmca.2010.2052605
17. Cheng, X.-Q., et al.: Application of linearization via state feedback to heading control for autonomous underwater vehicle. In: IEEE International Conference on Mechatronics and Automation. IEEE, pp. 477–482 (2008)
18. Sun, B., et al.: A novel fuzzy control algorithm for three-dimensional AUV path planning based on sonar model. J. Intell. Fuzzy Syst. 26(6), 2913–2926 (2014). https://doi.org/10.3233/ifs-130957
19. Wang, J., et al.: Command filter based adaptive neural trajectory tracking control of an underactuated underwater vehicle in three-dimensional space. Ocean. Eng. 180, 175–186 (2019). https://doi.org/10.1016/j.oceaneng.2019.03.061
20. Zhang, Z., Wu, Y.: Adaptive fuzzy tracking control of autonomous underwater vehicles with output constraints. IEEE Trans. Fuzzy Syst. 29(5), 1311–1319 (2021). https://doi.org/10.1109/tfuzz.2020.2967294
21. Yu, C., et al.: Guidance-error-based robust fuzzy adaptive control for bottom following of a flight-style AUV with saturated actuator dynamics. IEEE Trans. Cybern. 50(5), 1887–1899 (2020). https://doi.org/10.1109/tcyb.2018.2890582
22. Kazemi, S., Geranmehr, B., Nekoo, S.R.: Finitary optimal gain for diving control of AUVs via input-state linearization. In: 5th RSI International Conference on Robotics and Mechatronics, IcRoM 2017, pp. 292–297 (2018)
23. Zhu, D., Sun, B.: The bio-inspired model based hybrid sliding-mode tracking control for unmanned underwater vehicles. Eng. Appl. Artif. Intell. 26(10), 2260–2269 (2013). https://doi.org/10.1016/j.engappai.2013.08.017
24. Peng, Y., et al.: Research on hover control of AUV uncertain stochastic nonlinear system based on constructive backstepping control strategy. IEEE Access. 10, 50914–50924 (2022). https://doi.org/10.1109/access.2022.3169587
25. An, S., et al.: Adaptive backstepping sliding mode tracking control for autonomous underwater vehicles with input quantization. Adv Theory Simul. 5(4), 1–9 (2022). https://doi.org/10.1002/adts.202100445
26. Zhang, G.C., et al.: A novel adaptive second order sliding mode path following control for a portable AUV. Ocean. Eng. 151, 82–92 (2018). https://doi.org/10.1016/j.oceaneng.2017.12.054
27. Chen, B., et al.: Finite-time velocity-free observer-based consensus tracking for heterogeneous uncertain AUVs via adaptive sliding mode control. Ocean. Eng. 23, 109565 (2021). https://doi.org/10.1016/j.oceaneng.2021.109565
28. Zong, G., Sun, H., Nguang, S.K.: Decentralized adaptive neuro-output feedback saturated control for INS and its application to AUV. IEEE Transact. Neural Networks Learn. Syst. 32(12), 5492–5501 (2021). https://doi.org/10.1109/tnnls.2021.3050992
29. Fang, K., et al.: Neural adaptive output feedback tracking control of underactuated AUVs. Ocean. Eng. 23, 109211 (2021). https://doi.org/10.1016/j.oceaneng.2021.109211
30. Hodgkin, A., Huxley, A.F.: A quantitative description of membrane current and its application to conduction and excitation in nerve. J. Physiol. 117(4), 500–544 (1952). https://doi.org/10.1113/jphysiol.1952.sp004764
31. Yang, S.X., Meng, M.: An efficient neural network approach to dynamic robot motion planning. Neural. Network. 13(2), 143–148 (2000). https://doi.org/10.1016/s0893-6080(99)00103-3
32. Yang, S.X., Meng, M.Q.: Real-time collision-free motion planning of a mobile robot using a neural dynamics-based approach. IEEE Trans. Neural. Network. 14(6), 1541–1552 (2003). https://doi.org/10.1109/tnn.2003.820618
33. Yang, S.X., Meng, M.: Neural network approaches to dynamic collision-free trajectory generation. IEEE Trans. Syst. Man Cybern. B Cybern. 31(3), 302–318 (2001). https://doi.org/10.1109/3477.931512
34. Yang, X., et al.: Disturbance observer based on biologically inspired integral sliding mode control for trajectory tracking of mobile robots. IEEE Access. 7, 48382–48391 (2019). https://doi.org/10.1109/access.2019.2907126
35. Xu, Z., et al.: Backstepping and sliding mode control for AUVs aided with bioinspired neurodynamics. In: IEEE International Conference on Robotics and Automation (ICRA), pp. 2113–2119 (2021)
36. Soylu, S., Buckham, B.J., Podhorodeski, R.P.: A chattering-free sliding-mode controller for underwater vehicles with fault-tolerant infinity-norm thrust allocation. Ocean. Eng. 35(16), 1647–1659 (2008). https://doi.org/10.1016/j.oceaneng.2008.07.013
37. Lapierre, L., Jouvencel, B.: Robust nonlinear path-following control of an AUV. IEEE J. Ocean. Eng. 33(2), 89–102 (2008). https://doi.org/10.1109/joe.2008.923554
38. Grossberg, S.: Nonlinear neural networks: principles, mechanisms, and architectures. Neural. Network. 1(1), 17–61 (1988). https://doi.org/10.1016/0893-6080(88)90021-4
39. Sun, B., Zhu, D., Yang, S.X.: A novel tracking controller for autonomous underwater vehicles with thruster fault accommodation. J. Navig. 69(3), 593–612 (2016). https://doi.org/10.1017/s0373463315000806

How to cite this article: Xu, Z., et al.: A hybrid tracking control strategy for an unmanned underwater vehicle aided with bioinspired neural dynamics. IET Cyber-Syst. Robot. 4(3), 153–162 (2022). https://doi.org/10.1049/csy2.12060